Water Air Soil Pollut (2018) 229: 260
https://doi.org/10.1007/s11270-018-3911-1

Retention and Transport of Bisphenol A and Bisphenol S in Saturated Limestone Porous Media

Yanfeng Shi · Yuanyuan Sun · Bin Gao · Hongxia Xu · Xiaoqing Shi · Jichun Wu

Received: 7 March 2018 / Accepted: 9 July 2018 / Published online: 24 July 2018

Abstract The release of bisphenols such as bisphenol A (BPA) and its alternative bisphenol S (BPS) into the subsurface environment may cause serious pollutions to soil and groundwater. However, only few works have examined their fate and transport in porous media. In this work, batch and column experiments and mathematical modeling were conducted to study the transport behaviors of BPA and BPS in water-saturated limestone porous media. The effects of contaminant input concentration, solution ion type, and solution ionic strength on the retention and transport of BPA and BPS in the columns were investigated. BPS had higher mobility in limestone porous media than that of BPA. With its input concentration decreased, BPA showed lower mobility, while the transport of BPS in the media was not affected by the input concentration perturbations. The retention of both BPA and BPS was higher in divalent calcium ion solution than that in monovalent sodium solution in limestone porous media. Ionic strength showed little effect on the retention and transport of BPA and BPS except that high concentration of Ca^{2+} inhibited the migration of BPS in the media. Because of its relatively high mobility and toxicity, BPS may present a great risk to groundwater quality and thus may not be an environmentally friendly bisphenol alternative.

Keywords Bisphenol A · Bisphenol S · Fate and transport · Adsorption · Limestone porous media

1 Introduction

Bisphenol A (BPA; 4,4-isopropylidene diphenol) is a chemical intermediate used primarily in the manufacture of polycarbonate products and epoxy resins, which are widely used in plastics, food packing, and thermal receipts (Staples et al. 1998). In recent years, the world production of the BPA has increased rapidly and is forecasted to reach 10.6 million metric tons by 2022 (Report Code CP021 2016). BPA is a known endocrine disruptor which is harmful to environment and public health. Its exposure may lead to various serious diseases, such as breast cancer, prostate cancer, neuroendocrinology disease, metabolism disorder, and obesity (Chen et al. 2016; Diamanti-Kandarakis et al. 2009; Rochester 2013). Therefore, some restrictions and legislations have been introduced to the use of BPA worldwide recently (Baluka and Rumbeiha 2016; Erler and Novak 2010). With the growing awareness of the toxicity and the use limitations of BPA, alternatives such as

Electronic supplementary material The online version of this article (https://doi.org/10.1007/s11270-018-3911-1) contains supplementary material, which is available to authorized users.

Y. Shi · Y. Sun (✉) · H. Xu · X. Shi · J. Wu (✉)
Key Laboratory of Surficial Geochemistry of Ministry of Education, School of Earth Sciences and Engineering, Hydrosciences Department, Nanjing University, Xianlin Campus, Xianlin Boulevard 163, Nanjing 210023, China
e-mail: sunyy@nju.edu.cne-mail: jcwu@nju.edu.cn

B. Gao
Department of Agricultural and Biological Engineering, University of Florida, Gainesville, FL 32611, USA

bisphenol S (BPS, 4,4′-sulfonyldiphenol) and bisphenol F are increasingly used in commercial products (Choi and Lee 2017; Liao et al. 2012). BPS, whose molecular structure is similar to that of BPA, is an organic compound composed of two phenol groups connected by a sulfone group (SO_2), instead of a branched three carbon group that connects the two phenol (Russo et al. 2017). It may exhibit estrogenic or genotoxic activities similar to BPA even at very low concentrations (Chen et al. 2016; Rosenmai et al. 2014). BPA and BPS may be released directly or indirectly into the environment during the manufacture, usage, and disposal of polycarbonate and epoxy resins and plastic products (Huang et al. 2012). They have been detected frequently in groundwater, surface water, landfill leachate, soil, sediment, and even in the blood and urinary of human beings around the world (Corrales et al. 2015; Im and Loffler 2016; Jin and Zhu 2016; Liao et al. 2012; Lin et al. 2017; Rosenmai et al. 2014; Vandenberg et al. 2007; Wu et al. 2017; Yang et al. 2014). The occurrence of BPA and BPS in the environment has posed great risks to public health; therefore, it is necessary to investigate their fate and transport in subsurface.

The retention of BPA/BPS in the porous media is one of the most important processes which strongly affects their transport and fate in subsurface. Some researchers have evaluated the sorption of BPA in soils or sediments through batch sorption experiments with controlled physicochemical factors (Sun et al. 2012; Sun et al. 2009; Xu et al. 2008). It has been reported that decrease of pH, temperature, and salinity can increase the sorption of BPA on sediments (Xu et al. 2008). The sorption of BPA on sediments also increases with rising ion concentration and Ca^{2+} has a greater influence on the adsorption process of BPA than Na^{+} (Sun et al. 2009). In addition, the sorption capacities of soils and sediments to BPA are positively correlated to their organic carbon contents (Sun et al. 2012). Previous studies have also demonstrated that both black carbon and organic matters in soils can increase the adsorption of BPA (Cunha et al. 2012; Toledo et al. 2005; Xu et al. 2008; Zeng et al. 2006). However, there is little information about the sorption behaviors of BPS in the soils or sediments, even though it is a popular bisphenol alternative (Guo et al. 2016).

In comparison to the batch sorption method, column transport experiment is more suitable for the evaluation of the fate and transport of contaminants in subsurface. Li et al. conducted soil column experiments to study the retention and release of BPA and found that the presence of higher ionic strength, heavy metals, and cationic surfactants can increase the BPA adsorption (Li et al. 2008). Using column experiments and mathematical model, Zakari et al. examined the transport behaviors of BPA at different pore-water velocities and initial input concentrations and found that BPA transported 0.11–0.83 m/day in the sandy sediment column with the water velocity of 1 m/day (Zakari et al. 2016). Nevertheless, the information and knowledge of the fate and transport of bisphenols such as BPA and BPS in soils and groundwater system are still limited. Further studies on the fate and transport of BPA and BPS in porous media thus are critical to understand their environmental impacts and potential risks.

The transport of organic pollutants in groundwater depends on the properties of not only the compounds and the flow (e.g., ionic strength and pH), but also the media (i.e., the aquifer materials) (Banzhaf and Hebig 2016). Nevertheless, previous studies on the fate and transport of organics including bisphenols have only used porous media such as sand, soils, and sediments. Little is known about the transport and fate of organic compounds in the limestone porous media. Limestone is a sedimentary rock composed of the mineral calcite (calcium carbonate), which makes up about 10% of the total volume of all sedimentary rocks (Kogel 2006). It has a wide distribution in the world, such as karst area and calcareous soil. Some research has found that the limestone has a wide range of surface potential with both positive and negative values which is different from the sand (Alotaibi et al. 2011; Alroudhan et al. 2016; Chen et al. 2014). It is thus of great interest to study the transport and fate of BPA/BPS in the limestone porous media.

This work investigated the transport behavior of BPA and BPS in limestone porous media. Laboratory experiments and numerical simulations were conducted under different solution chemistry conditions. The overall objectives were as follows: (1) determine the influence of input concentration on the transport of BPA/BPS in saturated limestone porous media; (2) determine the effects of solution ion type and ionic strength on the sorption and transport of BPA/BPS in the media; and (3) test mathematical models for simulating the fate and transport of BPA/BPS in the media.

2 Materials and Methods

2.1 Materials

BPA and BPS with purity of 99.5% were purchased from Sigma Chemicals. Basic physical and chemical properties of BPA and BPS are displayed in Table S1. To prepare the BPA stock solution (100 mg/L), BPA was first dissolved in methanol and then diluted by deionized (DI) water. The volume ratio of methanol to water was below 0.1% (*v*/*v*) in order to avoid the cosolvent effect (Zhou et al. 2014). The BPS stock solution (100 mg/L) was prepared by dissolving BPS directly in DI water. The stock solutions were stored in the refrigerator at 4 °C and were diluted with DI water to the desired concentrations prior to each use. Sodium chloride (1.0 mM, 20.0 mM, 50.0 mM) and calcium chloride (0.3 mM, 6.7 mM, 16.7 mM) were used in the experiments to test the effects of ion type and ionic strength.

Limestone was collected from an outcrop in Hengyang County, Hunan Province, China. It was crushed and sieved into the size ranged from 0.6–0.9 mm as the limestone porous media (granular material of limestone composition) and washed sequentially with tap and DI water to remove impurities, followed by oven drying at 40 °C for 48 h (Bayat et al. 2015). Mineral composition of the limestone was analyzed by X-ray diffraction (XRD, DMX-IIIA, Japan) with the Cu kα radiation (λ = 0.154 nm) and a step size of 0.02° in the 2θ range from 3 to 51°. The surface morphology and elemental composition of the limestone were determined with a scanning electron microscope equipped with energy dispersive X-ray (SEM-EDX, JEOL JSM-6490, Japan). The major surface elements of limestone were also detected by an X-ray fluorescence (XRF, ARL-9800, Switzerland). The Brunauer-Emmett-Teller (BET) surface area of the limestone was measured by a Micropore & Chemisorption Analyzer (ASAP 2020 HD88, Micromeritics) with eight-point nitrogen pressured ranged from 0.05–0.2 and pretreatment of degassed 10 h at 105 °C. The organic content of the limestone was detected by an Elemental Analyzer (ECS 4024 CHNSO, Costech Inc., Italy). The surface functional groups of the limestone were detected by Fourier Transform Infrared Spectrometer (FTIR, NICOLET6700, Nicolet Continuum Microscope). The zeta potentials of limestone under varying solution chemistry conditions were conducted using a Zeta PALS analyzer (Brookhaven Instruments Corporation, NY, USA).

2.2 Batch and Column Experiments

2.2.1 Batch Experiments

The adsorption kinetics, adsorption isotherm, and desorption experiments were carried out to determine the adsorption behaviors of BPA/BPS onto the limestone porous media. For all batch experiments**,** the BPA/BPS solutions were adjusted by NaCl and $CaCl_2$ to have the ionic strength with 1, 20, and 50 mM, respectively. An accurate weighing of 2.0 g limestone grains and 20 mL of the BPA/BPS solutions were mixed in 40 mL polytetrafluoroethylene (PTFE) tubes and shaken in the mechanical shaker at 125 rpm and 25 °C. For the sorption kinetic experiments, the limestone porous media with BPA and BPS (5 mg/L) were shaken for 0.02, 0.08, 0.17, 0.33, 1.00, 3.00, 6.00, 12.00, and 24.00 h, respectively. For the adsorption isotherm experiments, a series of initial concentrations of BPA (0.5, 2, 5, 10, 20, 50 mg/L) and BPS (1, 5, 20, 50, 100 mg/L) solutions adjusted by NaCl and $CaCl_2$ were mixed with limestone porous media and shaken 24 h to achieve equilibration. Desorption experiment were conducted using the post-sorption limestone samples from the isotherm experiments. The solid samples were rinsed with the working electrolyte solution without any BPA/BPS. All of the liquid samples from the batch experiments were collected and filtered by the PTFE filter (0.22 μm). The BPA and BPS concentrations in each of the liquid samples were analyzed by a high-performance liquid chromatography (HPLC, Agilent 1100, Agilent Technologies, Co., California, USA) with a DAD detector, at the wavelength of 227 nm and 258 nm respectively. The HPLC system is equipped with a C18 column (150 mm × 4.6 mm, Thermo Fisher, Hypersil GOLD). The samples with 100 μL injection volume were eluted by methanol/water (68/32 and 47/53 *v*/*v* for BPA and BPS, respectively) at a velocity of 1.0 mL/min. At the same time, the pH of part of the liquid samples was tested with a Thermo ORION STAR A215 pH/Conductivity Meter which was calibrated before each used. The batch experiments of BPA/BPS were carried out in triplicate including blank and control samples.

2.2.2 Column Experiments

Column experiments were conducted in PTFE columns (12-cm length and 2.5-cm inside diameter) (Dong et al. 2017). Stainless-steel mesh (50 μm) was placed at each

end of the column to hold the limestone porous media and to make the flow uniformly. The limestone grains were wet-packed into the column in order to avoid air entrapment as the saturated porous media. The porosity of each column was about 0.435. A high-precision syringe pump (Sigma Aldrich Corp., St. Louis, MO) with a glass syringe connected to the columns by PTFE tubing was used to introduce the desired electrolyte solution at a constant Darcy velocity of 0.204 cm/min (flow rate of 1.0 mL/min). Before each experiment, all the columns were firstly flushed with DI water for about 10 pore volumes (PVs) to remove impurities, followed by five PVs of background solution for hydrochemical equilibration. The BPA/BPS solution of different solution chemistry (Table 2) was then introduced into the inlet of columns as a pulse (50 mL, ~2 PVs) by the syringe pump at the same constant flow rate. After that, the column was flushed with the background solution for 13 PVs. Effluent samples were collected in glass tubes from the outlet of the columns with a fraction collector (BS-100A, Puyang Scientific Instrument Research Institute, China) at every 4-min intervals. The collected samples were filtered by a PTFE filter (0.22 μm) and analyzed immediately by the HPLC for BPA/BPS concentrations and the pH meter for pH values. KNO_3 (25 mg/L) was used as the conservative tracer under the same conditions. Nitrate (NO^{3-}) concentrations were detected by a UV-2000 Spectrophotometer (UNICO Instrument Co., ltd. China) at the wavelength of 220 nm (Dong et al. 2017). The breakthrough curves obtained from the plotted normalized effluent concentration (the ratio of effluent samples concentration and input concentrations, C/C_0) versus time. All the column experiments were conducted in duplicate at the temperature of 25 °C.

2.3 Mathematical Model

2.3.1 Langmuir Model

The Langmuir (Eq. (1)) adsorption model was applied to analyze the sorption isotherms of the BPA/BPS onto the limestone.

$$q_e = \frac{C_e K_l q_m}{1 + C_e K_l} \tag{1}$$

where q_e (mg/kg) is equilibrium adsorbed concentrations of the solid; C_e (mg/L) is the concentration of the aqueous; K_l and q_m are the Langmuir adsorption coefficient and the maximum adsorption capacity.

2.3.2 Two-Site Kinetic Model

Two-site kinetic model (attachment and detachment model) was used to simulate BPA/BPS transport in the limestone porous media columns (Simunek and van Genuchten 2008; Teijón et al. 2014; Zakari et al. 2016). The governing equations that base on the advection-dispersion equation (ADE) are defined as:

$$\frac{\partial C}{\partial t} + \frac{\rho}{\theta}\frac{\partial S_1}{\partial t} + \frac{\rho}{\theta}\frac{\partial S_2}{\partial t} = D\frac{\partial^2 C}{\partial z^2} - v\frac{\partial^2 C}{\partial z} \tag{2}$$

$$\frac{\rho}{\theta}\frac{\partial S_1}{\partial \mathrm{t}} = k_1 C \tag{3}$$

$$\frac{\rho}{\theta}\frac{\partial S_2}{\partial t} = k_2 C - k_{d2}\frac{\rho}{\theta}S_2 \tag{4}$$

where C is the concentration in the aqueous phase (M/L^3); t is time (T); ρ is the bulk density of limestone porous media (M/L^3); θ is the volumetric water content; S_1 and S_2 are the solid phase solute concentration-associated site 1 and site 2, respectively (M/M); D is the hydrodynamic dispersion coefficient (L^2/T); z is the coordinate parallel to flow (L); v is the velocity of pore water (L/T); k_1 and k_2 are the attachment coefficients for site 1 and site 2, respectively (T^{-1}), and k_{d2} is the detachment coefficient for site 2 (T^{-1}).

The two-site kinetic model was used to simulate the transport experiment data by inverse fitting of k_1, k_2, and k_{d2} using the HYDRUS-1D software (Simunek et al. 1998). The dispersion coefficient (D) was obtained from inverse fitting of the experimental breakthrough curves (BTCs) of the tracer.

3 Results and Discussion

3.1 Characterization

The XRD image (Fig. S1) shows that the mineralogy of limestone porous media used in this study was mainly calcite with a small amount of dolomite and quartz. SEM images (Fig. S2a, b) indicate that the limestone porous media had a rough surface with full of irregular

bumps and dents. Therefore, there is a high possibility that the remained BPA and BPS became trap inside the porous medium. The BET surface area of the limestone porous media was 0.5921 m^2/g, which is relatively large at the grain size of 0.6–0.9 mm. The rough surface and relatively large surface area might promote the adsorption and retention of the BPA and BPS onto the limestone porous media. The EXD analysis results (Fig. S2c) show that element of limestone surface was mainly calcium (wt% 18.5), oxygen (wt% 57.7), carbon (wt% 16.5), and a low content of silicon and other metal elements (magnesium, aluminum, and potassium). The X-ray fluorescence results (Table S2) show that the limestone porous media was mainly CaO (wt% 48.8) with small amount of SiO_2, MgO, Al_2O_3, and K_2O, which are consistent with the XRD and EDX conclusions that the major element of the limestone media was calcium, with some silicon, magnesium, aluminum, and other elements. In addition, the limestone porous media used in this work contained very low level organic carbon (wt% 0.08). In the FTIR spectra of the limestone porous media (Fig. S3), absorption peaks at 714, 876, 1441, and 2513 cm^{-1} were ascribed to $CaCO_3$ (El-Sherbiny et al. 2015). Carboxyl (absorption peaks appearing at 1734 cm^{-1}) and hydroxyl (absorption peaks appearing at 3622 cm^{-1}) groups were also found on the limestone porous media (Dong et al. 2017).

The zeta potential of limestone porous media generally decreases with the increasing solution pH; however, it increases with the increasing of the cation (e.g., Ca^{2+} and Na^+) concentrations (Alroudhan et al. 2016; Chen et al. 2014; Kasha et al. 2015). In this work, the zeta potential of the limestone porous media in different electrolyte solutions increased from − 12.60 to − 3.11 (mV) and from − 1.34 to 9.02 (mV) with the increasing of the concentrations of NaCl and $CaCl_2$, respectively (Table S3). Alotaibi et al. reported that surface-charge (zeta potential) adjustment from negative to positive can alter the wettability of carbonate rock from preferentially water-wet to oil-wet (Alotaibi et al. 2011). High Ca^{2+} concentration in the solution made the limestone porous media more hydrophobic (or less hydrophilic) in this work and thus could potentially promote the adsorption of BPA/BPS onto the limestone porous media surface.

3.2 Batch Experiments

Sorption kinetic results of BPA and BPS onto limestone porous media showed that their sorption rates from fast to slow and reached equilibrium within 24 h (Fig. S4). In comparison to that of BPS, the sorption of BPA onto the limestone porous media was higher under different ion type and ionic strength conditions (Fig. 1). The Langmuir results fitted the experimental isotherms well with $R^2 > 0.99$. The maximum sorption capacity (Q_{max}) and K_1 of BPA are greater than those of BPS under the same ion type and ionic strength conditions (Table 1). In addition, the desorption experiment indicated that the desorption of BPS from the limestone porous media was lower than that of BPA (Fig. S5). This may be attributed to the fact that BPA and BPS have different molecular structures (Table S1). The intermediates connecting the two phenols of BPA and BPS are propyl and sulfone, respectively. Because the sulfone group of the BPS has strong

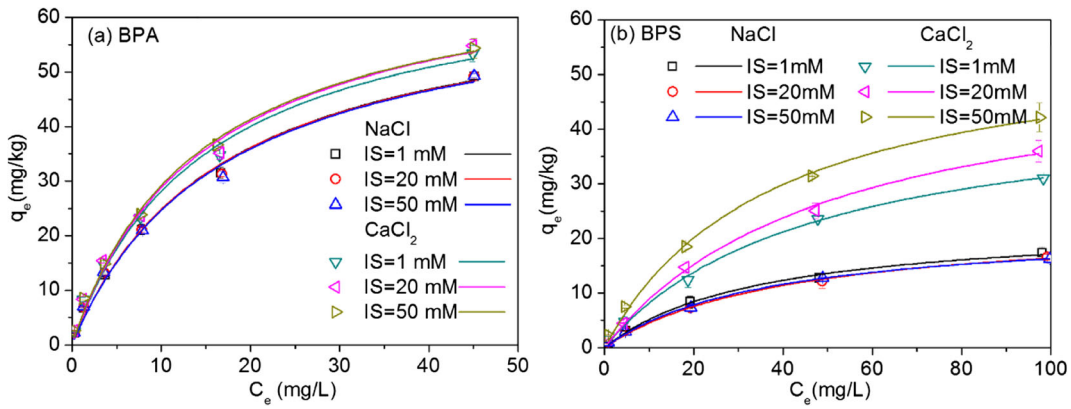

Fig. 1 Adsorption isotherms of **a** BPA and **b** BPS onto limestone porous media in different ionic solutions (NaCl and $CaCl_2$). Error bars represent standard deviations of replicate experiments under all conditions ($n = 3$). Symbols and lines represent experimental and model results, respectively

Table 1 Isotherm fitting parameters for BPA and BPS adsorption by limestone in different solution

Solution	BPA Langmuir			BPS Langmuir		
	Q_{max}	K_l	R^2	Q_{max}	K_l	R^2
IS = 1 mM (NaCl)	66.63	0.06	0.99	23.08	0.03	0.99
IS = 20 mM(NaCl)	66.29	0.06	0.99	23.19	0.02	0.99
IS = 50 mM(NaCl)	66.38	0.06	0.99	22.24	0.03	1.00
IS = 1 mM ($CaCl_2$)	69.64	0.07	0.99	45.61	0.02	0.99
IS = 20 mM($CaCl_2$)	71.33	0.07	0.99	54.12	0.02	1.00
IS = 50 mM($CaCl_2$)	70.79	0.07	0.99	57.83	0.03	1.00

electron-withdrawing ability than propyl group of the BPA, the solubility (1774 mg/L) of BPS is much higher than that of BPA (120 mg/L) (Choi and Lee 2017; Staples et al. 1998). In addition, the BPS has a lower logKow value (logKow = 1.65) than BPA (logKow = 3.40), indicating BPS is less hydrophobic (Choi and Lee 2017). Therefore, the BPA with lower solubility has a stronger tendency to be adsorbed onto the organic matters of the limestone porous media (Choi and Lee 2017; Sun et al. 2012; Zhou et al. 2014). The difference in molecular structures also makes the two compounds have different pK_a values (Table S1). The pK_{a1}、pK_{a2} values of the BPA are 9.6 and 10.2, higher than the corresponding values of the BPS (7.4 and 8.0). Under tested conditions in this work (pH 8.6–9.8), most of the BPA was in either uncharged or partially negatively charged (i.e., one of the two hydroxyl groups was deprotonated) forms; while BPS was mainly in either partially negatively charged or fully negatively charged (i.e., two hydroxyl groups were deprotonated) form. The hydroxyl groups of the uncharged BPS compound and the partially charged BPS and BPA compounds might interact with the oxygen-containing groups of the limestone porous media through hydrogen bond or hydrophobic interactions to promote the adsorption (Jing et al. 2012; Zhou et al. 2014). However, for most of the tested conditions (except in Ca^{2+} solutions), the limestone porous media surfaces were also negatively charged. The electrostatic repulsion interactions might hinder the adsorption of the partially negatively charged compounds (especially BPS) onto the limestone porous media.

In comparison to Na^+, Ca^{2+} in the solutions promoted the adsorption of BPA and BPS onto the limestone porous media (Fig. 1 and Table 1). This was probably caused by following two factors: (1) the presence of Ca^{2+} in the solution changed the surface potential of the limestone porous media from negative into positive, which might introduce the electrostatic attraction of charged BPA/BPS onto the limestone porous media surface, and (2) as a divalent cation, Ca^{2+} might act as "cation bridges" to promote the deposition of negatively charged BPA/BPS onto negatively charged limestone porous media surface. Similar effects of ion type (Ca^{2+} vs. K^+) on BPA adsorption on soils have been observed in previous studies (Sun et al. 2005).

Ionic strength had little effect on the adsorption of BPA onto the limestone porous media (Fig. 1a and Table 1), confirming the importance of hydrogen bond and hydrophobic interactions to BPA adsorption under the tested conditions. For similar reason, ionic strength also showed little influences on BPS adsorption on limestone porous media in Na^+ solution. However, BPS adsorption increased with increasing Ca^{2+} (Fig. 1b and Table 1), which is consistent with the previously proposed mechanisms that the presence of Ca^{2+} increased electrostatic attraction of negatively charged BPS to limestone porous media through altering the surface charge of the media or providing cation bridges.

3.3 Effect of Input Concentration on BPA/BPS Transport

The results of the nonreactive tracer test showed the limestone porous media were well-packed in the columns without notable signs of preferential flow paths or "wall effects," and the dispersivity (0.1087 cm) was obtained by fitting the tracer result (Table 2). The BTCs show that BPS has higher mobility than BPA under the same experimental conditions (Fig. 2). Mass balance calculations show that the total recovery rates of BPS in the effluents were 84.11–90.37%, much higher than those of BPA (36.69–72.68%) under the same conditions (Table 2). These results suggest that BPS was more mobile in the limestone porous media than BPA, which is consistent with isotherm data that the adsorption BPA onto limestone porous media was higher than that of BPS.

When the input concentration of BPA increased from 1 to 25 mg/L, its recovery also increased from 36.69 to 72.68% (Table 2). In addition, the initial breakthrough time of BPA also reduced with the increasing input concentration. These results suggest that the adsorption of BPA onto the limestone porous media relied on the availability of the adsorption sites (e.g., amount of surface function groups). When the input concentration increased,

Table 2 Fitting parameters of the two-site kinetic model for BPA and BPS transport in limestone porous media at varying electrolyte solution and concentration

Compound	Concentration (mg/L)	IS (mM)		Effluent recovery (%)	D_{isp}[a] (cm)	k_1[b] (min^{-1})	k_2[b] (min^{-1})	k_{d2}[b] (min^{-1})	R^2
		NaCl	$CaCl_2$						
BPA	1	1	–	36.69	0.1087	0.0394	0.1517	0.0312	0.81
	5	1	–	50.42	0.1087	0.0316	0.1105	0.0774	0.95
	5	20	–	55.89	0.1087	0.0291	0.1232	0.0850	0.93
	5	50	–	55.90	0.1087	0.0291	0.1045	0.0712	0.93
	5	–	1	46.41	0.1087	0.0354	0.1615	0.0599	0.88
	5	–	20	47.78	0.1087	0.0341	0.1638	0.0539	0.83
	5	–	50	45.14	0.1087	0.0376	0.1850	0.0651	0.85
	25	1	–	72.68	0.1087	0.0181	0.0821	0.1053	0.96
BPS	1	1	–	85.91	0.1087	0.0082	0.0922	0.3128	0.99
	5	1	–	84.11	0.1087	0.0085	0.0454	0.1713	1.00
	5	20	–	84.36	0.1087	0.0080	0.0531	0.1877	0.99
	5	50	–	80.65	0.1087	0.0096	0.0563	0.1658	0.99
	5	–	1	58.45	0.1087	0.0247	0.0579	0.0775	0.98
	5	–	20	49.41	0.1087	0.0287	0.0615	0.0559	0.97
	5	–	50	44.28	0.1087	0.0358	0.1067	0.0798	0.96
	25	1	–	90.37	0.1087	0.0041	0.0760	0.2847	1.00

D_{isp}, k_1, k_2, and k_{d2} represent longitudinal dispersivity, first-order sorption coefficient and desorption coefficient on site 1, first-order sorption coefficient on site 2, respectively. R^2 represents the squared Pearson correlation coefficient

[a] Parameter determined from tracer experiments

[b] Parameter determined from BPA/BPS experiments

the adsorption sites were filled quickly to reduce the further retention of BPA in the limestone porous media, which is called as the "blocking effect" (Kasel et al. 2013). Blocking is a process that occurs when adsorbates attached to a surface of porous media reduce the area (or site) available for attachment of other adsorbates to the surface (Camesano et al. 1999). This "blocking" effect has also been observed for the retention and transport of other contaminants in saturated porous media (Sun et al. 2015). For BPS, however, its BTCs showed little changes with the input concentrations (Fig. 2b), probably because the amount of adsorbed BPS was too little to cause the

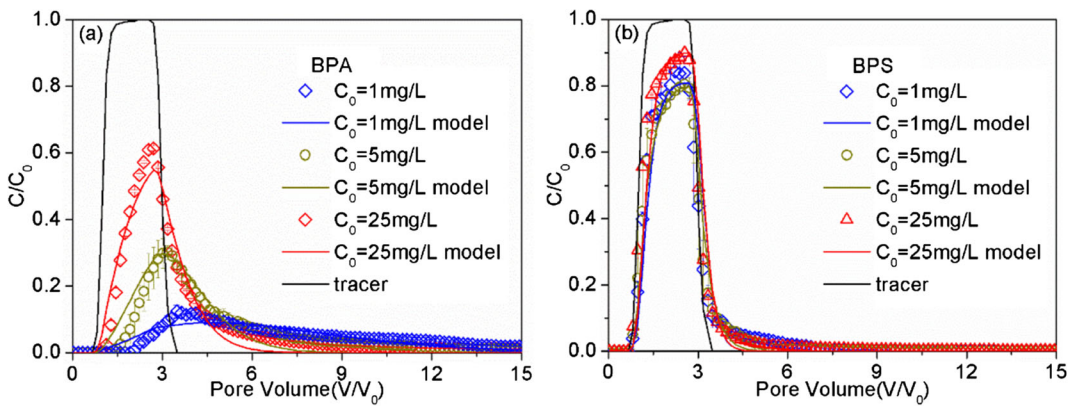

Fig. 2 Breakthrough curves of different concentration **a** BPA and **b** BPS in the limestone porous media. C and C_0 represent the concentration of effluent and influent, respectively. Error bars represent standard deviations of replicate experiments under all conditions ($n = 2$)

blocking effect. The mass recovery rates of BPS in the column effluents were very high with values ranged from 84.11 to 90.37% for all the tested conditions (Table 2).

Although the two-site kinetic model does not consider the blocking effect, it described the BTCs of both BPA and BPS under different input concentrations very well (Fig. 2). The best-fit k_1 and k_2 values of BPA in the limestone porous media columns decreased with increasing input concentrations (Table 2), which might be attributed to the blocking effect as the two model parameters are constants reflecting the average deposition rates. For BPS in the columns, the best-fit k_1 and k_2 values did not change much with the increasing of input concentration, confirming the insignificance of blocking effect on the retention and transport of BPS in saturated limestone porous media. The best k_1 and k_2 values of BPA were 0.0181–0.0394 min^{-1} and 0.0821–0.1517 min^{-1}, respectively, which are higher than the corresponding values of BPS in the columns (0.0041–0.0085 and 0.0454–0.0922 min^{-1}, respectively). This confirms that BPS was more mobile than BPA in the columns.

3.4 Effect of Electrolyte Solution on BPA/BPS Transport

In comparison to that of Na^+, the presence of Ca^{2+} reduced the transport of BPA and BPS through the limestone porous media columns (Figs. 3 and 4). Mass balance calculations show that the recovery rates of BPA in Na^+ and Ca^{2+} solutions were 50.42–55.90% and 45.14–47.78%, respectively (Table 2). For BPS, the recovery rates in Na^+ and Ca^{2+} solutions were 80.65–84.36% and 44.28–58.45%, respectively (Table 2). When the other conditions are the same, both BPA and BPS showed lower BTCs and mass recovery rates in Ca^{2+} solutions than in Na^+ solutions. This indicate that Ca^{2+} increased retention of the two compounds in saturated limestone porous media, which is consistent with adsorption results that Ca^{2+} increased BPA and BPS adsorption onto the limestone porous media.

For the same ion type, changes in ionic strength showed little effect on the retention and transport of BPA in saturated limestone porous media (Fig. 3). This is consistent with the findings of the batch adsorption experiments (Fig. 1). The mass recovery rates of BPA in effluents of the columns were 50.42–55.90% and 45.14–47.78% in Na^+ and Ca^{2+} solutions, respectively (Table 2). Because BPA was mainly in uncharged and partially charged forms, its adsorption onto the limestone porous media was mainly through hydrogen bond and hydrophobic interactions. Increasing solution ionic strength thus had insignificant influences on its retention and transport in the media. For BPS in Na^+ solutions, ionic strength also showed little effect on its retention and transport in saturated limestone porous media (Fig. 4a) and mass recovery rates were 80.65–84.36% (Table 2), which was also due to the dominance of the hydrogen bond and hydrophobic interaction mechanisms. Increasing in ionic strength of Ca^{2+}, however, clearly reduced the transport of BPS in saturated limestone porous media (Fig. 4b). When the ionic strength of Ca^{2+} increased from 1 to 50 mM, the recovery rate of BPS reduced from 58.45 to 44.28% (Table 2), consistent with the adsorption experimental results that Ca^{2+} could

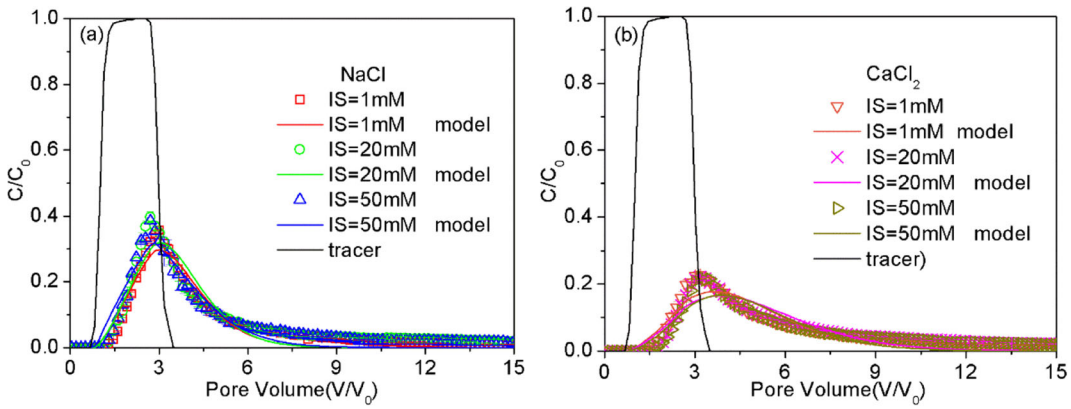

Fig. 3 Breakthrough curves of BPA in the limestone porous media under different electrolyte solution (**a** NaCl and **b** $CaCl_2$). C and C_0 represent for BPA concentration of effluent and influent, respectively. Error bars represent standard deviations of replicate experiments under all conditions ($n = 2$)

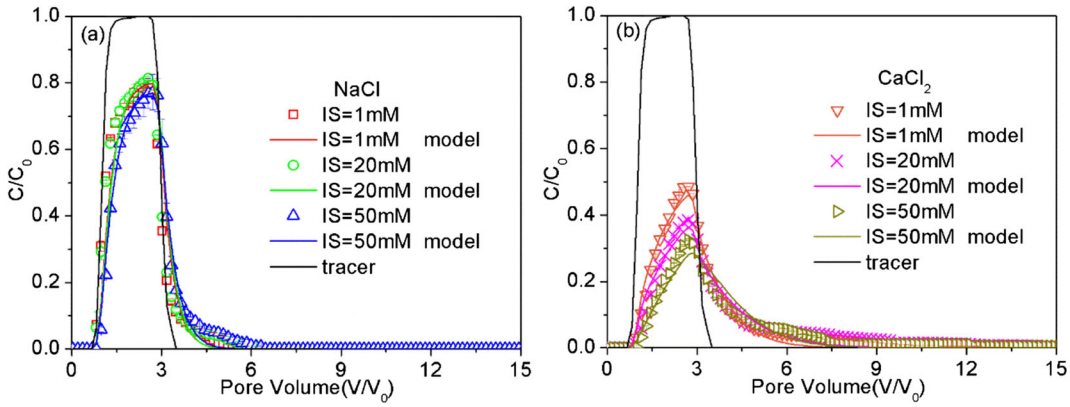

Fig. 4 Breakthrough curves of BPS in the limestone porous media under different electrolyte solution (**a** NaCl and **b** $CaCl_2$). C and C_0 represent for BPS concentration of effluent, influent, respectively. Error bars represent standard deviations of replicate experiments under all conditions ($n = 2$)

enhance the deposition of negatively charged BPS onto limestone porous media via the electrostatic attraction and cation bridge mechanisms.

Simulations of the two-site kinetic model also matched the experimental BTCs very well (Figs. 3 and 4) with R^2 values larger than 0.83 (Table 2). The best-fit k_1, k_2, and k_{d2} values of BPA were 0.0341–0.0376, 0.1615–0.1850, and 0.0539–0.0651 min^{-1} in Ca^{2+}, respectively; and 0.0291–0.0316, 0.1045–0.1232, and 0.0712–0.0850 min^{-1} in Na^+, respectively (Table 2). In comparisons to the corresponding values of BPA, the best-fit k_1 and k_2 values of BPS were smaller but the k_{d2} values were slightly larger, which are consistent with experimental results that BPS had higher mobility than BPA. The best-fit k_1, k_2, and k_{d2} values of BPS were 0.0247–0.0358, 0.0579–0.1067, and 0.0559–0.0798 min^{-1} in Ca^{2+}, respectively, and 0.0080–0.0096, 0.0454–0.0563 and 0.1658–0.1877 min^{-1} in Na^+, respectively (Table 2). In general, the k_1 and k_2 values of Ca^{2+} for both BPA and BPS were larger than the corresponding ones of Na^+; while the k_{d2} values of Ca^{2+} were smaller than the corresponding ones of Na^+. These results confirm that Ca^{2+} promoted the retention of both compounds in saturated limestone porous media.

4 Conclusions

Results of the batch adsorption and column transport experiments provide an insight into the dynamics and mechanisms of the retention and transport of BPA/BPS in saturated limestone porous media. All the experimental and modeling evidences suggest that BPA had lower mobility than BPS under various conditions because of the higher adsorption of BPA to the limestone porous media. In comparison to Na^+, the divalent cation Ca^{2+} promoted the adsorption of BPA/BPS onto the limestone porous media and thus reduced their transport in the media. In Na^+ solutions, ionic strength showed little effect on the retention and transport of BPA/BPS. In addition, blocking effect due to increasing input concentration was observed for BPA transport in the limestone porous media, but it was not obvious for that of BPS. Hydrogen bond and hydrophobic interactions might play governing roles in controlling the adsorption and retention of the two compounds, especially uncharged BPA, under the tested conditions; while electrostatic attraction and cation bridges introduced by Ca^{2+} might also contribute to the adsorption and retention of negatively charged BPA/BPS in the media. Findings from this study can improve current understanding of bisphenol fate and transport in the subsurface environment, and thus help making accurate assessment of their potential environmental risks.

Funding Information This work was financially supported by the National Natural Science Foundation of China-Xianjiang project (U1503282), the National Natural Science Foundation of China (41372234), and the National Natural Science Foundation of Jiangsu Province (BK20151385).

References

Alotaibi, M. B., Nasr-El-Din, H. A., & Fletcher, J. J. (2011). Electrokinetics of limestone and dolomite rock particles. *SPE Reservoir Evaluation & Engineering, 14*(05), 594–603.

Alroudhan, A., Vinogradov, J., & Jackson, M. D. (2016). Zeta potential of intact natural limestone: impact of potential-determining ions Ca, Mg and SO_4. *Colloids and Surfaces A: Physicochemical and Engineering Aspects, 493*, 83–98.

Baluka, S. A., & Rumbeiha, W. K. (2016). Bisphenol A and food safety: lessons from developed to developing countries. *Food and Chemical Toxicology, 92*, 58–63.

Banzhaf, S., & Hebig, K. H. (2016). Use of column experiments to investigate the fate of organic micropollutants – a review. *Hydrology & Earth System Sciences Discussions, 2016*, 1–35.

Bayat, A. E., Junin, R., Derahman, M. N., & Samad, A. A. (2015). TiO_2 nanoparticle transport and retention through saturated limestone porous media under various ionic strength conditions. *Chemosphere, 134*, 7–15.

Camesano, T. A., Unice, K. M., & Logan, B. E. (1999). Blocking and ripening of colloids in porous media and their implications for bacterial transport. *Colloids & Surfaces A Physicochemical & Engineering Aspects, 160*(3), 291–307.

Chen, L., Zhang, G., Wang, L., Wu, W., & Ge, J. (2014). Zeta potential of limestone in a large range of salinity. *Colloids & Surfaces A Physicochemical & Engineering Aspects, 450(*1), 1–1), 8.

Chen, D., Kannan, K., Tan, H., Zheng, Z., Feng, Y. L., Wu, Y., & Widelka, M. (2016). Bisphenol analogues other than BPA: environmental occurrence, human exposure, and toxicity – a review. *Environmental Science & Technology, 50*(11), 5438–5453.

Choi, Y. J., & Lee, L. S. (2017). Partitioning behavior of bisphenol alternatives BPS and BPAF compared to BPA. *Environmental Science & Technology, 51*(7), 3725–3732.

Corrales, J., Kristofco, L. A., Steele, W. B., Yates, B. S., Breed, C. S., Williams, E. S., & Brooks, B. W. (2015). Global assessment of bisphenol A in the environment: review and analysis of its occurrence and bioaccumulation. *Dose-Response, 13*(3), 1–29.

Cunha, B. B., Botero, W. G., Oliveira, L. C., Carlos, V. M., Pompeo, M. L. M., Fraceto, L. F., & Rosa, A. H. (2012). Kinetics and adsorption isotherms of bisphenol a, estrone, 17 beta-estradiol, and 17 alpha-ethinylestradiol in tropical sediment samples. *Water Air & Soil Pollution, 223*(1), 329–336.

Diamanti-Kandarakis, E., Bourguignon, J. P., Giudice, L. C., Hauser, R., Prins, G. S., Soto, A. M., Zoeller, R. T., & Gore, A. C. (2009). Endocrine-disrupting chemicals: an Endocrine Society scientific statement. *Endocrine Reviews, 30*(4), 293–342.

Dong, S. N., Sun, Y. Y., Gao, B., Shi, X. Q., Xu, H. X., Wu, J. F., & Wu, J. C. (2017). Retention and transport of graphene oxide in water-saturated limestone media. *Chemosphere, 180*, 506–512.

El-Sherbiny, S., El-Sheikh, S. M., & Barhoum, A. (2015). Preparation and modification of nano calcium carbonate filler from waste marble dust and commercial limestone for papermaking wet end application. *Powder Technology, 279*, 290–300.

Erler, C., & Novak, J. (2010). Bisphenol a exposure: human risk and health policy. *Journal of Pediatric Nursing, 25*(5), 400–407.

Guo, H., Li, H., Liang, N., Chen, F., Liao, S., Zhang, D., Wu, M., & Pan, B. (2016). Structural benefits of bisphenol S and its analogs resulting in their high sorption on carbon nanotubes and graphite. *Environmental Science and Pollution Research, 23*(9), 1–9.

Huang, Y. Q., Wong, C. K. C., Zheng, J. S., Bouwman, H., Barra, R., Wahlstrom, B., Neretin, L., & Wong, M. H. (2012). Bisphenol A (BPA) in China: a review of sources, environmental levels, and potential human health impacts. *Environment International, 42*, 91–99.

Im, J., & Loffler, F. E. (2016). Fate of bisphenol A in terrestrial and aquatic environments. *Environmental Science & Technology, 50*(16), 8403–8416.

Jin, H. B., & Zhu, L. Y. (2016). Occurrence and partitioning of bisphenol analogues in water and sediment from Liaohe River Basin and Taihu Lake, China. *Water Research, 103*, 343–351.

Jing, X., Li, W., & Zhu, Y. (2012). Decontamination of bisphenol A from aqueous solution by graphene adsorption. *Langmuir, 28*(22), 8418–8425.

Kasel, D., Bradford, S. A., J, Š., Heggen, M., Vereecken, H., & Klumpp, E. (2013). Transport and retention of multi-walled carbon nanotubes in saturated porous media: effects of input concentration and grain size. *Water Research, 47*(2), 933–944.

Kasha, A., Al-Hashim, H., Abdallah, W., Taherian, R., & Sauerer, B. (2015). Effect of Ca^{2+}, Mg^{2+} and SO_4^{2-} ions on the zeta potential of calcite and dolomite particles aged with stearic acid. *Colloids and Surfaces A: Physicochemical and Engineering Aspects, 482*, 290–299.

Kogel, J. E. (2006). Industrial minerals & rocks: commodities, markets, and uses: SME.

Li, J., Zhou, B., Liu, Y., Yang, Q., & Cai, W. (2008). Influence of the coexisting contaminants on bisphenol A sorption and desorption in soil. *Journal of Hazardous Materials, 151*(2–3), 389–393.

Liao, C., Liu, F., & Kannan, K. (2012). Bisphenol s, a new bisphenol analogue, in paper products and currency bills and its association with bisphenol a residues. *Environmental Science & Technology, 46*(12), 6515–6522.

Lin, Z., Wang, L., Jia, Y., Zhang, Y., Dong, Q., & Huang, C. (2017). A study on environmental bisphenol A pollution in plastics industry areas. *Water, Air, & Soil Pollution, 228*(3), 98.

Report Code CP021. (2016). *Bisphenol-A – a global market overview*. (pp. 194).

Rochester, J. R. (2013). Bisphenol A and human health: a review of the literature. *Reproductive Toxicology, 42*, 132–155.

Rosenmai, A. K., Dybdahl, M., Pedersen, M., Wedebye, E. B., Taxvig, C., & Vinggaard, A. M. (2014). Are structural analogues to bisphenol a safe alternatives? *Toxicological Sciences, 139*(1), 35–47.

Russo, G., Barbato, F., & Grumetto, L. (2017). Monitoring of bisphenol A and bisphenol S in thermal paper receipts from the Italian market and estimated transdermal human intake: A pilot study. *Science of the Total Environment, 599–600*, 68–75.

Simunek, J., & van Genuchten, M. T. (2008). Modeling nonequilibrium flow and transport processes using HYDRUS. *Vadose Zone Journal, 7*(2), 782–797.

Simunek, J., Saito, H., Sakai, M., & Genuchten, T. M. (1998). The HYDRUS-1D software package for simulating the one-dimensional movement of water, heat, and multiple solutes in variably-saturated media (p. 68). Riverside: Dep. of Environmental Sciences Univ. of California Riverside.

Staples, C. A., Dorn, P. B., Klecka, G. M., O'Block, S. T., & Harris, L. R. (1998). A review of the environmental fate, effects, and exposures of bisphenol A. *Chemosphere, 36*(10), 2149–2173.

Sun, W. L., Ni, J. R., O'Brien, K. C., Hao, P. P., & Sun, L. Y. (2005). Adsorption of bisphenol A on sediments in the Yellow River. *Water Air & Soil Pollution, 167*(1–4), 353–364.

Sun, W. L., Ni, J. R., Li, T. H., Sun, L. Y., & Petticrew, E. L. (2009). Effect of Ca^{2+} and Na^{+} on the sorption of three selected endocrine disruptors to sediments. *Marine & Freshwater Research, 60*(7), 767–773.

Sun, K., Jin, J., Gao, B., Zhang, Z., Wang, Z., Pan, Z., Xu, D., & Zhao, Y. (2012). Sorption of 17α-ethinyl estradiol, bisphenol A and phenanthrene to different size fractions of soil and sediment. *Chemosphere, 88*(5), 577–583.

Sun, Y., Gao, B., Bradford, S. A., Lei, W., Hao, C., Shi, X., & Wu, J. (2015). Transport, retention, and size perturbation of graphene oxide in saturated porous media: effects of input concentration and grain size. *Water Research, 68*, 24–33.

Teijón, G., Candela, L., Šimůnek, J., Tamoh, K., & Valdes-Abellan, J. (2014). Fate and transport of naproxen in a Sandy aquifer material: saturated column studies and model evaluation. *Soil and Sediment Contamination, 23*, 736–750.

Toledo, I. B., Ferro-Garcia, M. A., Rivera-Utrilla, J., Moreno-Castilla, C., & Fernandez, F. J. V. (2005). Bisphenol A removal from water by activated carbon. Effects of carbon characteristics and solution chemistry. *Environmental Science & Technology, 39*(16), 6246–6250.

Vandenberg, L. N., Hauser, R., Marcus, M., Olea, N., & Welshons, W. V. (2007). Human exposure to bisphenol A (BPA). *Reproductive Toxicology, 24*(2), 139–177.

Wu, L., Zhang, X., Wang, F., Gao, C., Chen, D., Palumbo, J., Guo, Y., & Zeng, E. (2017). Occurrence of bisphenol S in the environment and implications for human exposure: a short review. *Science of the Total Environment, 615*, 87–98.

Xu, X. R., Wang, Y. X., & Li, X. Y. (2008). Sorption behavior of bisphenol A on marine sediments. *Journal of Environmental Science and Health Part A, 43*(3), 239–246.

Yang, Y., Guan, J., Yin, J., Shao, B., & Li, H. (2014). Urinary levels of bisphenol analogues in residents living near a manufacturing plant in south China. *Chemosphere, 112*, 481–486.

Zakari, S., Hui, L., Lei, T., Yan, W., & Liu, J. (2016). Transport of bisphenol-A in sandy aquifer sediment: column experiment. *Chemosphere, 144*, 1807–1814.

Zeng, G., Zhang, C., Huang, G., Yu, J., Wang, Q., Li, J., Xi, B., & Liu, H. (2006). Adsorption behavior of bisphenol A on sediments in Xiangjiang River, Central-south China. *Chemosphere, 65*(9), 1490–1499.

Zhou, X., Wei, J., Liu, K., Liu, N., & Zhou, B. (2014). Adsorption of bisphenol A based on synergy between hydrogen bonding and hydrophobic interaction. *Langmuir, 30*(46), 13861–13868.